

A charge separation system for the muon collider

R.C. Fernow & J.C. Gallardo
Brookhaven National Laboratory

28 February 2005

We examine systems for efficiently separating the positive and negative particles produced in the muon collider target. The beam first passes through a phase rotation system to maximize the number of particles in the momentum acceptance of the following linear 6D pre-cooler system. The charge separation is done with a large-aperture bent solenoid. The subsequent transport system produces two parallel beams, 5 m apart in the horizontal plane. The system produces $0.27 \mu^+ / p$ and $0.28 \mu^- / p$ in a standard longitudinal phase space box.

1. Introduction

A lot of progress has been made on understanding the beam dynamics and machine requirements for a muon collider [1,2]. However, a realistic, self-consistent design of the front end for a muon collider remains a major, unsolved problem. In this report we envision a front end that tries to collect all the muons into one or two bunches as soon as possible after the production target. Consider the possible configuration shown in Fig. 1.

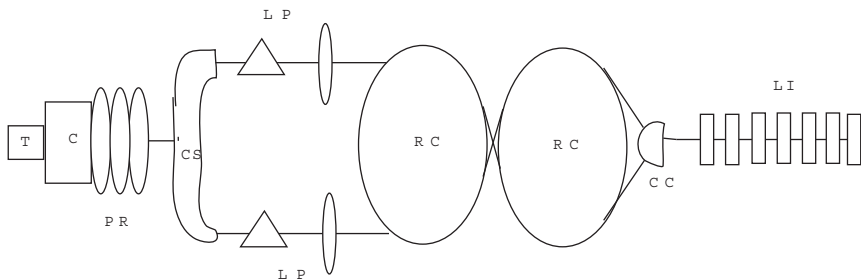


Figure 1. Possible layout for the front end of a muon collider.

Pions are produced by interactions of a proton driver beam with a high-power mercury target (T). The pions are collected with a high-field solenoid (C), whose strength quickly tapers down to a more moderate value. In this design the pions and muons first pass

through a phase rotation system (PR) to maximize the number of particles in the momentum acceptance of the following linear pre-cooler (LP) channels. Besides transverse cooling the pre-cooler channels must reduce the longitudinal emittance as quickly as possible. They must contain dispersive elements for emittance exchange and as a result separate channels must be provided for positive and negative charged particles. Thus we place a charge separation system (CS) in front of the pre-coolers. The charge separation is done here with a large-aperture bent solenoid. After a sufficient amount of pre-cooling the beams may be injected into a series of cooling rings (RC), as shown in Fig. 1, or into an alternative cooling system, such as a gas-filled helical channel. At some point the beams may be recombined (CC) and sent into a linear lithium lens channel (LI), for example, for ultimate transverse cooling.

It is important to reiterate that no solution for the front-end of a muon collider exists at this time. Until a complete solution is demonstrated we can only propose schemes based on promising subsystems and simulate how well the total system works. The scenario illustrated in Fig. 1 should be considered in this light. Many alternative ideas, such as gas-filled helical channels and coalescing a long bunch train, have been proposed and also need to be simulated in similar detail.

In this report we concentrate on the problem of efficiently separating the positive and negative particles leaving the phase rotation channel.

2. Phase rotation

The pion production was modeled using the program MARS [3]. The 39 m long phase rotation channel, which used high-gradient 40.25 MHz RF cavities, has been described in a previous note [4] and is shown in Fig. 2.

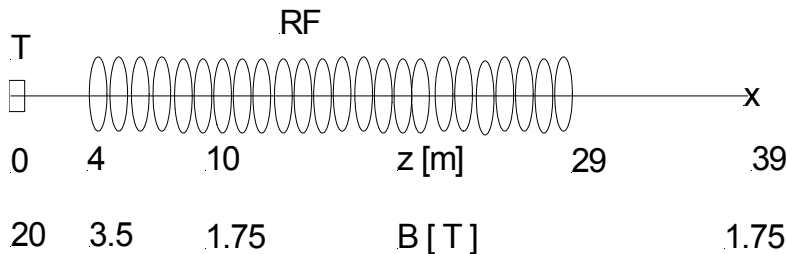


Figure 2. Schematic of the phase rotation system. T: target, RF: 40 MHz RF cavities.

The model is fairly realistic, including, for example, beryllium RF windows and periodic solenoids along the channel. Both positive and negative particles pass simultaneously through the cavities, separated in time by roughly half an RF wavelength. Fig. 3 shows the dependence of the number of particles at the end of the channel on the phase shift in the RF cavities.

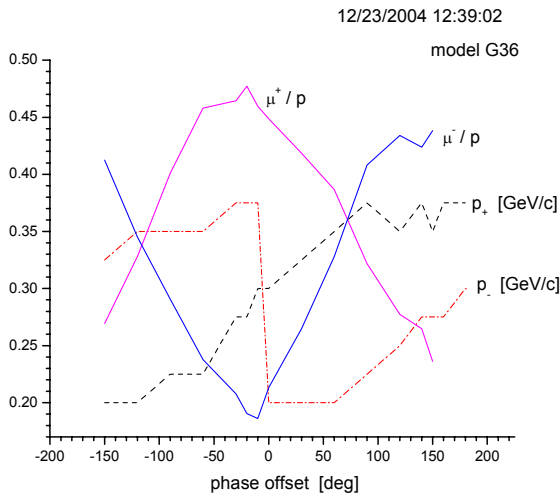


Figure 3. Flux and average momentum of positive and negative particles at the end of the phase rotation channel as a function of the phase shift in the RF cavities.

It seems desirable to have equal numbers of particles in the positive and negative bunches. There are two phase shifts that give the result. Note however from Fig. 3 that the two bunches with equal numbers of particles have different momenta. We choose to operate the channel at a phase shift of 71° , which produces a flux of $0.36 \mu/p$ (muons per incident proton on the target) at the entrance to the charge separation system.¹

This choice of how to run the phase rotation system is actually another of the many branch points in the design of a front-end system. The choice made here has two main advantages: (A1) Subsequent systems down to the collider should have approximately equal numbers of particles per bunch. As a result, hardware design, beam loading and instabilities should be similar for the two beams. (A2) This mode of operation gives both charges of particle beam for every proton driver pulse on target. However, this mode of operation also has two main disadvantages. (D1) The phase spaces of the two beams in the charge separation system are very different. The positive beam has higher momentum while the negative beam is spread out more in time. This makes it difficult to simultaneously optimize the charge separation system for both signs. (D2) The phase chosen does not give the maximum number of particles available from the phase rotation system.

There is an alternative mode of operation, which was adopted for the status report [1], where one proton driver pulse is dedicated to the positive charge beam and the following pulse is dedicated to the negative charges. This mode shares the feature (A1) and eliminates the two disadvantages listed above. However, the pulse repetition frequency in this mode is only 50%. At this point it is not clear which mode is better.

¹ These beam files and the other ICOOL files used in these simulations can be found at <http://pubweb.bnl.gov/people/fernaw/projects/MC310/>.

3. Charge separation configurations

We assume that the charge separation system must deliver the two beams to separate linear 6D precooling channels. We demand that the two channels be parallel to each other, and be in a plane roughly parallel to the surface of the earth. Since the precooler will almost certainly contain low frequency RF cavities, we also demand that the two channels be a reasonable distance, say ~ 5 m, apart. We want the final charge-separated beams to be as identical as possible. Thus the system should include some provision for reducing the momentum of the positive beam. We would also like to present the precooler with “clean” beams. Thus some provision must be included to remove the dispersion that must be introduced to do the charge separation.

The conventional method of charge separation uses a sequence of dipoles. However, since the phase rotator and most cooling designs use solenoidal focusing, it is more natural to use a bent solenoid to separate the charges [5]. Dispersion in a bent solenoid occurs in the direction perpendicular to the bending plane. The amount of dispersion is proportional to the total bend angle.

In the simulations we use a constant radial cut-off of 30 cm everywhere, except in the bent solenoid that does the actual charge separation. The charge separation bent solenoid needs a very large aperture to contain the incoming and outgoing beams. The charge separation bent solenoid does not use a superimposed dipole field, whereas all other bent solenoids used in the charge-separated transport lines do have a dipole field to keep the reference momentum on the system axis. All the bent solenoids have a curvature factor $h \sim 0.3$. The simulations described in this section were done with a “hard-edge” field model² and do not attempt to equalize the two beam momenta. More realistic field modeling is described in the following section. The charge separation bent solenoid has two circular holes of radius 30 cm in the exit plane. The centers of the holes are adjusted to match the mean transverse deflection of the two charges. The tails of the beams are lost getting into the holes and, in addition, there are substantial losses of particles with large divergences over the following few meters of the transport.

As a figure of merit we look at the number of particles at the end of the system that are enclosed in a rectangular box in longitudinal phase space. The box has a length of 6 m and a height of 200 MeV/c. These values were chosen to roughly take into account the maximum likely momentum acceptance and RF frequency (~ 40 MHz) of the precooler. The position of the box is varied to find the location with the maximum particle density.

We now examine some representative geometrical configurations for the charge separation system. We found that the transmission of the high momentum, positive beam is poor if the solenoid field is kept at the 1.75 T value used for the phase rotation channel. Thus all the configurations begin with a transition region (T) where the field is increased in strength. We found that a 3 T field gives reasonable performance. Increasing the solenoid above 3 T does not help because it causes the separation of the centers of the charge distributions at the exit plane to come too close together. Each configuration also

² This is done using BSOL model 1 in ICOOL, version 2.82 or later.

includes transition regions (T) in the output beamlines that return the solenoid field to 1.75 T.

3.1 Configuration 1

In the first configuration we bend the solenoid horizontally by 90° . At the end of this bent solenoid the two charges are diverging vertically, as shown in Fig. 4.

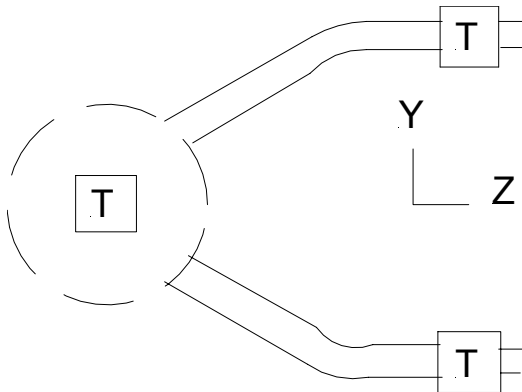


Figure 4. Bent solenoid configuration that separates the charges vertically. The beam enters the page on the left and bends by 90° in the horizontal plane. The two charge-separated beams travel from left to right at different heights. (model H23)

The beams leave the horizontal bent solenoid with a vertical divergence angle of 0.15 rad. We then use 11 m long straight solenoids to get the two beam 5 m apart. Finally vertical bent solenoids are used to get the two parallel beams into the horizontal plane. After these manipulations the two beams are stacked vertically.

The final box transmissions were ~ 0.29 for both signs of particles.

3.2 Configuration 2

In the second configuration, shown in Fig. 5, we use a shorter horizontal bent solenoid. The two charge-separated beams are then brought out horizontally.

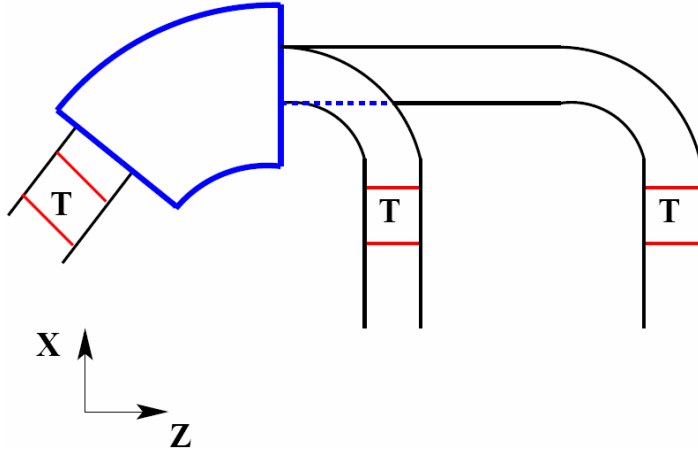


Figure 5. Bent solenoid configuration that separates the charges horizontally. The beam passes from left to right. The two charge-separated beams are at slightly different heights. (model H14)

The negative beam transport is made 5 m longer than the positive one. Then the two beams are sent through another horizontal bent solenoid that bends the beams by 90° . The end result is two beams separated by 5 m in the horizontal plane. The final box transmissions were ~ 0.25 for both signs of particles.

Although configurations 1 and 2 have reasonable transmission, they do not remove the dispersion introduced by the first bent solenoid. This can be seen, for example, for the positive particles in configuration 2 in Fig. 6.

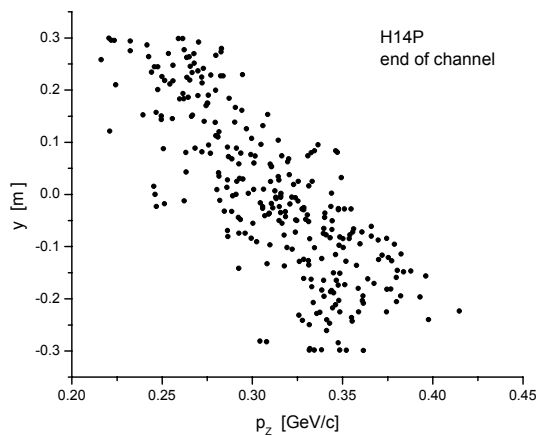


Figure 6. Vertical dispersion of positive beam for configuration 2.

Thus we must look for configurations where the second bend is in the same plane, but has the opposite sense as the first bent solenoid.

3.3 Configuration 3

Consider the configuration shown in Fig. 7. The beam is bent through 90 degrees in the horizontal plane and then separates vertically similar to configuration 1, except that here the second bend is also in the horizontal plane.

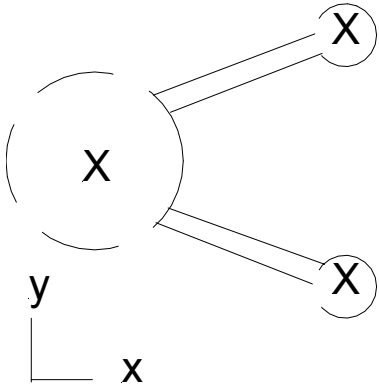


Figure 7. Bent solenoid configuration that separates the charges vertically. The beam enters perpendicular to the page on the left. (model H24)

The final beams are in the same direction as the initial beam, but are transversely offset from it. The final box transmissions were ~ 0.30 for the positive particles and ~ 0.28 for the negative particles. Most of the dispersion is removed from the final beams. Note that it is also possible to rotate this whole configuration by 90° around the incident beam direction. This would correspond to a vertical bent solenoid that bends the beams into the ground and produces two beams separated in the horizontal direction.

3.3 Configuration 4

Finally, let us consider a variation of configuration 2 where the second bend has the same magnitude, but opposite sense of the first bend, as shown in Fig. 8.

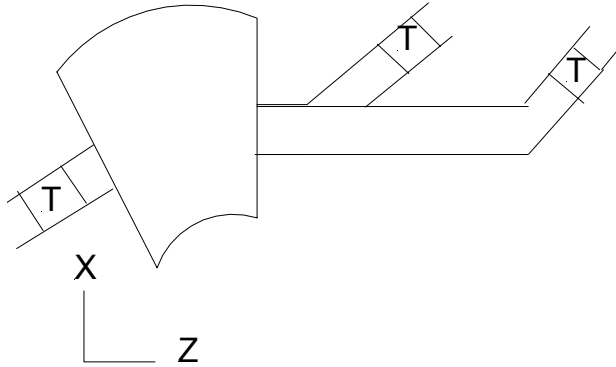


Figure 8. Bent solenoid configuration that separates the charges horizontally. The beam passes from left to right. (model H27)

The final beams are in the same direction as the initial beam, but are transversely offset from it. The final box transmissions were ~ 0.33 for the positive particles and ~ 0.32 for the negative particles. Most of the dispersion is removed from the final beams. This configuration gave the best performance. Note that it is also possible to rotate this whole configuration by 90° around the incident beam direction.

Properties of the four configurations are summarized in Table 1.

Table 1: Properties of charge separation systems

| conf | symm | Q | L [m] | Δy [cm] | B_D [T] | $r(p_z, y)$ | $\langle p \rangle$ [MeV/c] | TR_{BOX} |
|------|------|---|-------|-----------------|-----------|-------------|-----------------------------|-------------------|
| 1 | H V | + | 18.7 | -52 | -0.20 | -0.72 | 320 | 0.291 |
| | | - | 18.7 | 41 | 0.10 | 0.65 | 205 | 0.288 |
| 2 | H H' | + | 12.4 | -44 | 0.32 | -0.78 | 314 | 0.250 |
| | | - | 17.4 | 33 | -0.22 | 0.77 | 207 | 0.249 |
| 3 | H -H | + | 23.5 | -52 | -0.26 | 0.19 | 325 | 0.296 |
| | | - | 23.5 | 41 | 0.19 | 0.14 | 204 | 0.284 |
| 4 | H -H | + | 16.7 | -44 | -0.25 | 0.01 | 326 | 0.328 |
| | | - | 11.4 | 33 | 0.18 | 0.15 | 201 | 0.320 |

The second column gives the symmetry between the bending planes of the two bent solenoids. L is the total length of the channel, Δy is the distance of the center of the charge distribution from the midplane, B_D is the dipole field used in the second bent solenoid, r is the correlation coefficient between p_z and y (proportional to the vertical dispersion), $\langle p \rangle$ is the average beam momentum, and TR_{BOX} is the transmission into the standard longitudinal phase space box.

4. Realistic charge separation design

We will now use configurations 3 and 4 in the previous section for more realistic modeling. The new simulations include

- particle decay
- LiH absorber in high momentum line
- realistic field model

The length of the absorber was chosen so that the positive and negative beams had the same momentum (~ 200 MeV/c) at the end of the system. The bent solenoids were modeled by specifying a smoothly varying solenoid field $B_S(s)$, dipole field $B_Y(s)$ and curvature $h(s)$ along the axis³. ICOOL fits nearby grid points to a polynomial in order to interpolate values off the grid points and to obtain required s-derivatives analytically. The code uses a 3rd order solution of Maxwell's equations to obtain field values at off-axis points. As an example the on-axis fields and curvature used for the negative particles for configuration 4 are shown in Fig. 9.

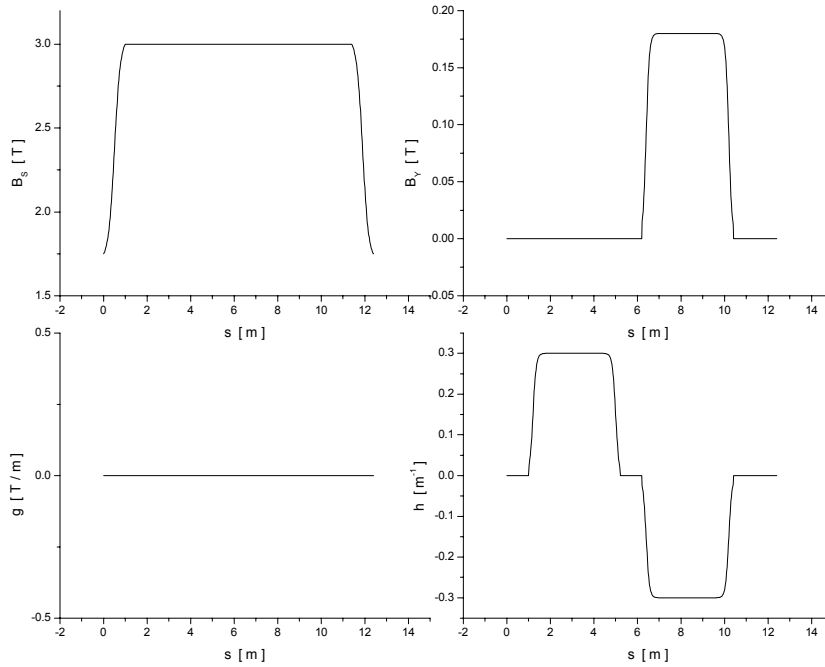


Figure 9. On-axis field and curvature used for realistic field modeling of the negative particles in configuration 4. B_S (upper left), B_Y (upper right), gradient (lower left), h (lower right).

We required the same geometrical curvature function for positive and negative particles in order to ensure the final beam channels were parallel.

³ This is done using BSOL model 3 in ICOOL, version 2.83 or later.

The layout of configuration 3 is shown in more detail in Fig. 10. A LiH absorber (A) was placed in the high-momentum (positive charge) line after the 90° bent solenoid.

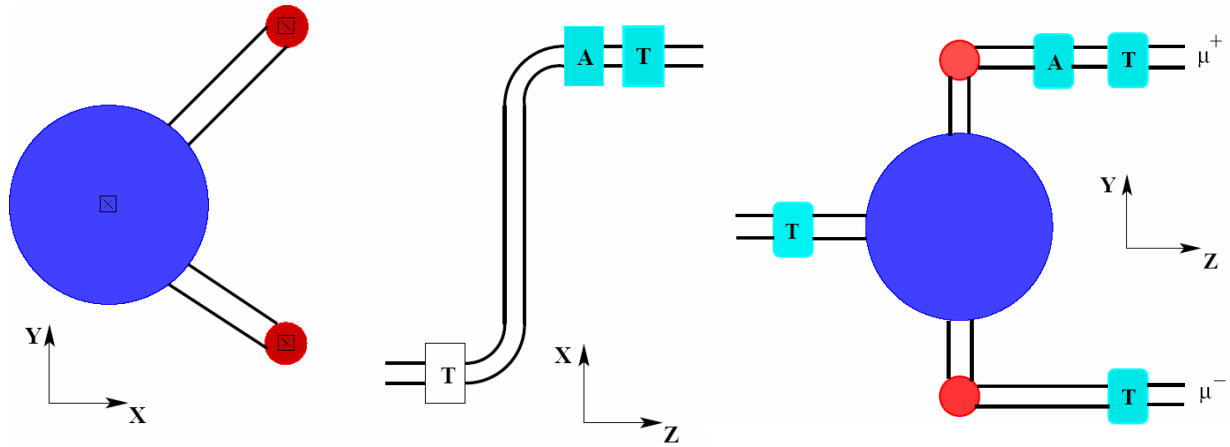


Figure 10. Three projections of realistic charge separation configuration 3. Transition regions (T) bring the solenoid field between 1.75 and 3 T. The LiH absorber (A) equalizes the momentum in the two beams.

The absorber had a trapezoidal shape and was 55 cm thick along the axis.

The modified layout of configuration 4 with the absorber (A) is shown in Fig. 11.

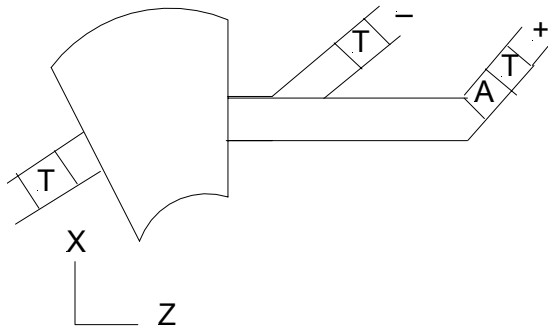


Figure 11. Schematic of realistic charge separation configuration 4. Transition regions (T) bring the solenoid field between 1.75 and 3 T. The absorber (A) equalizes the momentum in the two beams.

The absorber was a 75 cm long cylindrical block of LiH. Alternatively, a 44 cm long cylindrical block of beryllium could also be used to equalize the momenta.

Some important properties of the two systems are compared in Table 2.

Table 2: Comparison of realistic modeling

| conf | Q | L [m] | $r(p_z, y)$ | $\langle p \rangle$ [MeV/c] | Tr_{BOX} |
|------|---|-------|-------------|-----------------------------|-------------------|
| 3 | + | 24.5 | -0.01 | 206 | 0.192 |
| | - | 24.5 | 0.10 | 204 | 0.236 |
| 4 | + | 17.7 | 0.12 | 204 | 0.285 |
| | - | 12.4 | 0.11 | 205 | 0.305 |

The designs do a good job in equalizing the two beam momenta and in removing the dispersion. There is a significant drop in transmission compared with the hard-edge model in the previous section. Although the magnitudes of the curvature and dipole field were optimized, no attempt was made to optimize the shape of the on-axis fields. Configuration 4 has higher transmission and is shorter, so we adopt it as the standard design for the time being. The transverse phase space at the end of the channel is shown in Fig. 12.

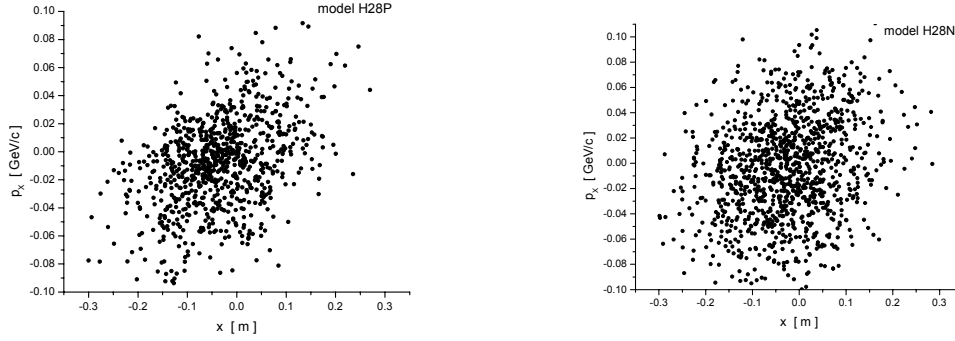


Figure 12. Transverse phase space at the end of the channel. Positive (left), negative (right).

The longitudinal phase space is shown in Fig. 13.

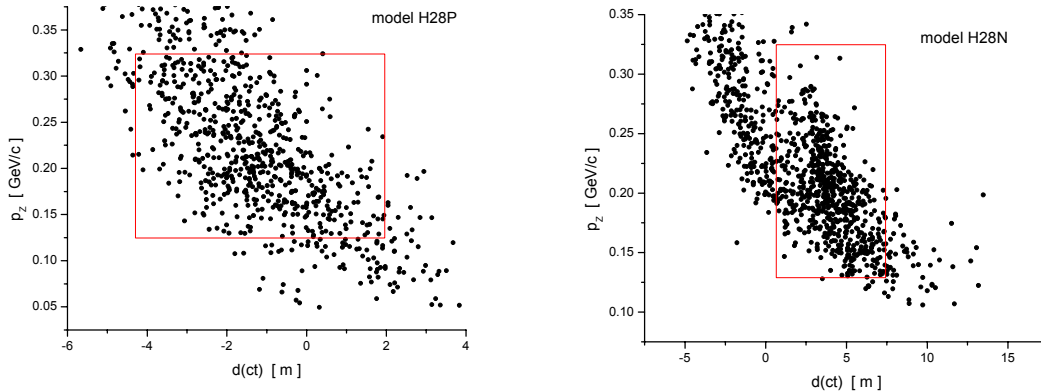


Figure 13. Longitudinal phase space at the end of the channel. Positive (left), negative (right). Both boxes have the same area.

Most of the positive particles fit in the standard phase space box, while the negative particles clearly do not. The negative particles have a much wider time spread.

Almost all of the dispersion is removed at the end of the channel. The vertical dispersion for the positive particles is shown in Fig. 14.

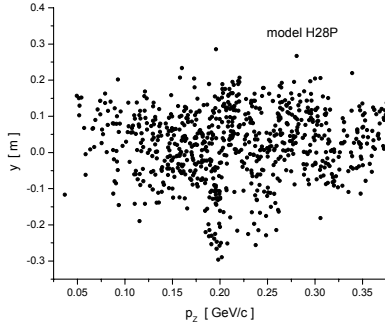


Figure 14. Dispersion at the end of the channel for positive particles.

Losses

It is instructive to examine where the particle losses occur in this system. Table 3 shows the overall transmission (TR) and the transmission into the standard longitudinal phase space box (TR_{BOX}) at several locations.

Table 3: Summary of losses in charge separation system

| location | + | | - | |
|----------|-------|-------------------|-------|-------------------|
| | TR | TR _{BOX} | TR | TR _{BOX} |
| start | 1.000 | 0.381 | 1.000 | 0.405 |
| BS hole | 0.893 | 0.365 | 0.900 | 0.366 |
| straight | 0.517 | 0.324 | 0.610 | 0.344 |
| 2nd BS | 0.506 | 0.319 | 0.583 | 0.314 |
| end | 0.416 | 0.285 | 0.576 | 0.305 |

Note that ~60% of the beam at the end of the phase rotation channel is in a “halo” outside the desired phase space box. Looking at TR we see that ~15% of the starting halo does not make it through the beam holes. This is illustrated in Fig. 15, which shows the distribution of particles at the bent solenoid exit plane.

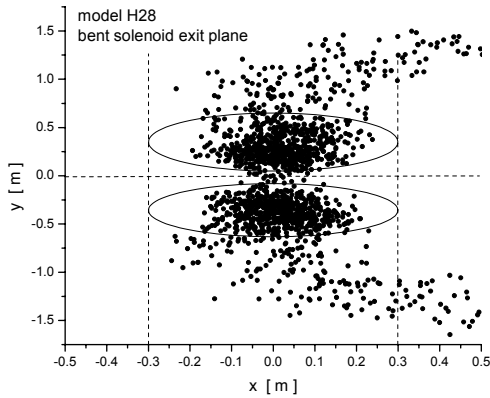


Figure 15. x-y distribution of particles at the exit plane of the charge separation bent solenoid. Positive (negative) particles have $y < 0$ ($y > 0$). The distorted “circles” show the exit holes.

In the beam core $\sim 93\%$ gets through the beam holes at the exit of the first bent solenoid. There are significant, roughly uniform losses in the remainder of the channel. At the end of the channel a significant halo still persists, particularly in the negative beam.

Normalization

This simulation started with beam particles from the exit of the phase rotation channel. Several normalization factors must be used to determine the number of muons per incident proton (μ / p) at the end of the charge separation channel. The first factor f_{TAR} is a weighting factor determined in the conversion of the MARS output file from the target into an equal-weight ICOOL input file. The second factor TR_{PR} is the probability that a particle in the ICOOL target beam file gets through the phase rotation channel. Finally the third factor TR_{BOX} is the probability that a particle that enters the charge separation channel is contained in the desired longitudinal phase space box at the end of the channel. Table 4 shows the relevant factors.

Table 4: Normalization factors

| Q | f_{TAR} | TR_{PR} | TR_{BOX} |
|---|------------------|-------------------------|--------------------------|
| + | 1.585 | 0.606 | 0.285 |
| - | 1.432 | 0.648 | 0.305 |

Using these normalization factors we can compute the number of accepted muons per incident proton. This is shown in Table 5 together with the normalized emittances for the accepted particles at the end of the charge separation channel.

Table 5: Beam summary at end of channels

| Q | ϵ_{TN} [mm] | ϵ_{LN} [mm] | $\langle p \rangle$ [MeV/c] | μ / p |
|---|-----------------------------|-----------------------------|-----------------------------|-----------|
| + | 21 | 420 | 204 | 0.274 |
| - | 23 | 380 | 205 | 0.283 |

These two beams must be accepted at the beginning of the first linear pre-cooler channels.

5. Prospects

The charge separation system described here has been modeled using realistic fields and reasonable assumptions about technical parameters. It is fairly efficient and produces two well-behaved beams. The next step will be to use these beams in a linear precooling channel. After the gap of 13-18 m without RF it may be necessary to begin the precooling using RF frequencies below 40 MHz. The 5 m separation between the two lines may be still be adequate using folded RF cavity designs, but whether this is possible with ~ 6 MV/m gradient is an open question.

Acknowledgements

We would like to thank Scott Berg for useful discussions.

References

- [1] C. Ankenbrandt et al, Status of muon collider research and development and future plans, Phys. Rev. Special Topics-Accelerators and Beams, 2, 081001 (1999).
- [2] M. Alsharo'a et al, Recent progress in neutrino factory and muon collider research within the Muon Collaboration, Phys. Rev. Special Topics-Accelerators and Beams, 6, 081001 (2003).
- [3] MARS was developed by Nikolai Mokhov. The beam file at the target used here was provided by Harold Kirk.
- [4] R. Fernow, Phase rotation for the muon collider, Muon Collaboration technical note MUC-NOTE-DECAY_CHANNEL-302, 12 November 2004.
- [5] N. Mokhov, R. Noble & A. Van Ginneken, Target and collection optimization for muon colliders, in Beam Dynamics and Technology Issues for $\mu^+ \mu^-$ Colliders, J. Gallardo (ed), AIP Conf. Proc. 372, p. 61, 1996.